

See discussions, stats, and author profiles for this publication at: <https://www.researchgate.net/publication/224969093>

# Mapping the influence of solubility and dielectric constant on electrospinning polycaprolactone solutions

ARTICLE · MAY 2012

---

CITATIONS

7

READS

49

## 3 AUTHORS:



[C. J. Luo](#)

University of Cambridge

13 PUBLICATIONS 343 CITATIONS

[SEE PROFILE](#)



[Eleanor Stride](#)

University of Oxford

179 PUBLICATIONS 2,616 CITATIONS

[SEE PROFILE](#)



[Mohan Edirisinghe](#)

University College London

154 PUBLICATIONS 2,222 CITATIONS

[SEE PROFILE](#)

## Mapping the Influence of Solubility and Dielectric Constant on Electrospinning Polycaprolactone Solutions

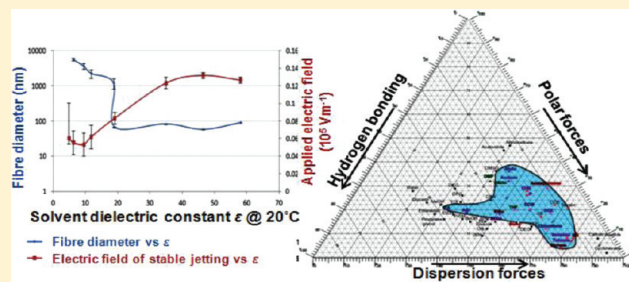
C. J. Luo,<sup>\*,†</sup> E. Stride,<sup>†,‡</sup> and M. Edirisinghe<sup>†</sup>

<sup>†</sup>Department of Mechanical Engineering, University College London, Torrington Place, London WC1E 7JE, U.K.

<sup>‡</sup>Institute of Biomedical Engineering, Department of Engineering Science, Old Road Campus, University of Oxford, Oxford OX3 7DQ, U.K.

 Supporting Information

**ABSTRACT:** Solvent–polymer interactions critically influence not only the viscoelasticity and the critical minimum solution concentration required for electrospinning but also the diameter, crystallinity, tensile strength, aspect ratio, and morphology of the electrospun fibers. Hence, a good understanding of the solvents and nonsolvents available and electrospinnable for a polymer of interest is important. The electrospinnability–solubility map uniquely presents the solubility and the electrospinnability of all solvents for a polymer in a single figure. Poly( $\epsilon$ -caprolactone) (PCL), an important polymer in biomedical applications, has been electrospun in a few conventional solvent systems, but a comprehensive mapping of its solvents for electrospinning has not been performed. Based on 49 common solvents of diverse solubility parameters and functional groups, the spinnability–solubility graph for electrospinning PCL solutions was mapped for the first time to enable a comprehensive understanding of the processability of all solvent choices for electrospinning PCL solutions. Furthermore, to date, many studies have demonstrated the importance of the dielectric constant (relative permittivity) of solvents in solution electrospinning, but few have systematically investigated its influence for a broad range of solvent systems. Based on the comprehensive PCL solvent map, this work studies the influence of dielectric constant of solvent systems on the electrospinning of PCL solutions. PCL ( $M_n = 80\,000$  g/mol) fiber diameters  $<100$  nm were achieved when the dielectric constant of a solvent system was  $\sim 19$  and above, below which fibers or relics of diameters from submicrometer to millimeter range were produced. A detailed investigation was carried out on solvent systems with a calculated range of dielectric constants by mixing acetic acid and formic acid—two solvents with significantly different dielectric constants but the same functional group and comparable in other physical properties influential in electrospinning. With increasing dielectric constant, the required applied voltage to achieve stable jetting increased, the frequency of bead-on-string morphology decreased, and the interfiber spacing increased without affecting the total mass of fibers spun per unit time. In addition, the dissolution and electrospinnability of poor or nonsolvents of PCL were tested at temperatures  $10\text{ }^\circ\text{C}$  or higher than the ambient temperature. A unique and novel morphology of electrospun fibers within electrosprayed relics was generated for the first time when electrospinning PCL in 2-ethoxyethyl acetate, a nonsolvent at an ambient temperature of  $20\text{--}22\text{ }^\circ\text{C}$  and a partial solvent of PCL at an elevated temperature of above  $30\text{ }^\circ\text{C}$ .



### 1. INTRODUCTION

Solvent systems are integral to drug development and pharmaceutical technology.<sup>1</sup> As polymer–solvent interactions determine the conformation of the polymer chain in a solution, the polymer solution properties are significantly affected by the solubility of the solvent.<sup>2</sup> Manipulations of solvent solubility influence not only the solution electrospinnability, viscoelasticity, and the critical minimum concentration of the solution in electrospinning but also the diameter, crystallinity, tensile strength, aspect ratio, and morphology of the electrospun polymeric fibers.<sup>3–10</sup> Solvent solubility was used to change the tensile strength of the as-spun fibers in flash spinning, which extrudes a polymer solution under increased pressure that enables dissolution of the polymer in a liquid that is a nonsolvent of the polymer at atmospheric conditions.<sup>11,12</sup> Furthermore, preferential solvent–polymer interactions alone

can be used to produce core–sheath fibers.<sup>13</sup> Mixing poly(methyl methacrylate) (PMMA) and polyacrylonitrile (PAN) in dimethylformamide (DMF) resulted in a metastable solution with a preferential dissolution of PAN to PMMA in DMF. The resulting emulsion produced PMMA-core/PAN-sheath nanofibers when directly electrospun in a single nozzle.<sup>13</sup>

An electrospinnability–solubility map based on the Teas graph uniquely presents the solubility and the electrospinnability of all solvents for a polymer in a single figure, without clustering the solvents into a three-dimensional diagram.<sup>3</sup> The proportions of solvent components in a mixed solvent system that provide the desired degree of dissolution and

Received: March 31, 2012

Revised: May 8, 2012

Published: May 18, 2012

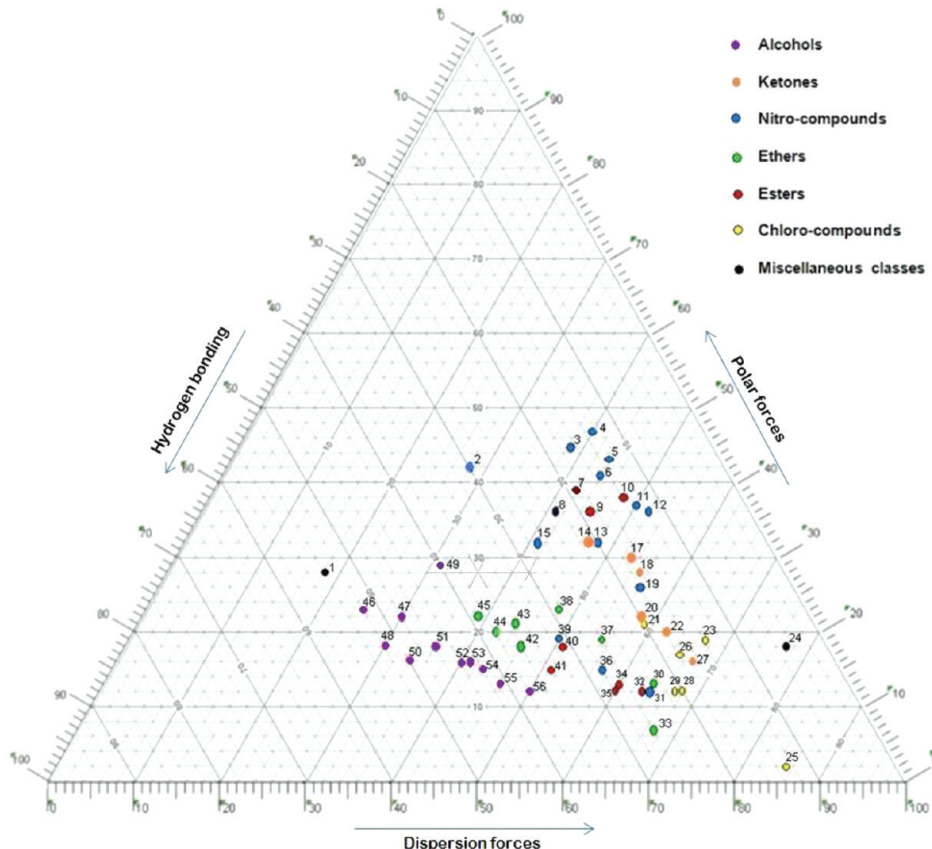


**Figure 1.** The Teas graph, a ternary fractional parameter solubility diagram. Solvent positions are colored according to classes showing the clustering of solvents of the same chemical group. Supporting Information and Table S1 provide further information on solubility mapping and the solvents listed in the figure.

electrospinnability can be geometrically analyzed on the 2D triangular map. Solvents of distinctive chemical groups and different solubility parameter zones have defined fractional solubility parameters, giving each solvent a fixed position on the map and providing a visual indication of the dispersion forces, the polar forces, and the hydrogen bonding of the solvent (Figure 1). Variations in the strengths of the three major molecular interactions of a solvent influence polymer–solvent interactions and consequently play an important role in enhancing or hindering electrospinning. Solvent mapping allows the overlapping of the solubility of different polymers onto one diagram and enables prediction of selective solvent solubility for a polymer blend or the mixing of different solvents at topographically calculated proportions to achieve a desirable selective solubility and electrospinnability for polymers of interest. This is useful for developing polymer emulsion blends by creating solvent systems with preferential solubility for one of the multiple polymers being mixed.

Much research has been done on electrospinning poly( $\epsilon$ -caprolactone) (PCL) solutions in several solvent systems for a broad range of biomedical applications.<sup>14–21</sup> However, the electrospinnability–solubility map has not been developed for this important polyester, which has been extensively investigated for tissue engineering and regenerative medicine. PCL is a semicrystalline bioerodible polymer. It is readily soluble in a large range of organic common solvents and hydrolyses under physiological conditions into water-soluble monomers. Both PCL and its monomer  $\epsilon$ -caprolactone are currently regarded as biocompatible and nontoxic.<sup>22</sup> Electrospun PCL structures are

suitable for biomedical applications such as 1 year implantable contraceptive devices, degradable staples for wound closures, long-term drug delivery systems (over 1 year), and tissue engineering.<sup>14,17,22–24</sup>

The spinnability of a polymer solution is related to the viscoelasticity of the process, particularly the ability of the polymer solution to be spun without breaking.<sup>25–27</sup> To achieve this, a polymer solution must have a critical minimum concentration  $c_e$  to allow sufficient molecular chain entanglements.<sup>28,29</sup> Insufficient chain entanglements lead to the formation of droplets and “bead-on-string” fiber morphology. The value of  $c_e$  and the degree of chain entanglement in a polymer solution are strongly influenced by the polymer molecular chain length and the conformation of the polymer chain in solution. The latter is closely associated with the intermolecular interactions between the polymer chain and the solvent molecules. At a constant temperature, the degree of this polymer–solvent intermolecular interaction defines the concept of solvent quality in general polymer solution rheology.<sup>30</sup> A polymer solution in a solvent of high solubility favors polymer–solvent interaction, as the polymer chains swell and expand to maximize intermolecular interaction. A polymer solution in a solvent of poor solubility favors polymer–polymer self-interactions, and the polymer chains contract and stay close to each other.<sup>30</sup> Solvent quality is affected by both temperature and the chemical compositions of the polymer and the solvent.

To date, many studies have indicated the importance of the solvent’s dielectric constant ( $\epsilon$ , also known as relative permittivity) in solution electrospinning.<sup>3,9,17,31,32</sup> However, few studies have

Table 1. List of Major Solvents and Their Physical Properties

solvent	$M_w$	bp (°C)	$\epsilon$ at 20 °C	dipole	electrical conductivity at 25 °C (S m <sup>-1</sup> )	latent heat (kJ mol <sup>-1</sup> )	surf. tension at 20 °C (mN m <sup>-1</sup> )	abs viscosity at 25 °C (mPa s)
acetic acid	60	118	6.2	1.7	$6.0 \times 10^{-7}$	24.3	27.4	1.13
acetone	58	56	20.6	2.9	$5.0 \times 10^{-7}$	29.6	23.3	0.33
acetonitrile	41	81.6	37.5	3.2	$6.0 \times 10^{-8}$	29.8	29.1	0.38
aniline	93	184	6.7	1.56	$2.4 \times 10^{-6}$	44.4	45.5	4.4
BuAc	116	126	5.01	1.8	$1.6 \times 10^{-6}$	35.9	25.1	0.73
chloroform	119	61	4.8	1.15	$<1.0 \times 10^{-8}$	29.4	27.16	0.57
cyclohexanone	98	156	18.2	3.1	$5.0 \times 10^{-16}$	37.7	34.5	2.2
DCM	85	40	9.1	1.8	$4.3 \times 10^{-9}$	28.1	28.12	0.44
DEG	106	245	31.7	2.31	$6.0 \times 10^{-5}$	66.5	48.5	34
diacetone alcohol	116	168	18.2 (25 °C)	3.24			31.0	2.9
DMAc	87	166	37.8	3.8		43.3	34	0.92
DMF	73	153	36.7	3.8	$6.0 \times 10^{-6}$	42.1	35	0.82
DMSO	78	189	46.6	3.96	$2.0 \times 10^{-7}$	52.9	43.7	2.0
EtAc	88	77	6.02	1.7	$1.0 \times 10^{-7}$	32.4	24	0.46
EDC	99	83.5	10.45	1.8	$4.0 \times 10^{-9}$	31.9	32.2	0.9
EtOH	46	78	22.4	1.7	$1.4 \times 10^{-7}$	38.5	22.3	1.08
2-ethoxyethanol	90	135	5.3	1.69	$9.3 \times 10^{-6}$	39.9	28.2	2.5
2-ethoxyethyl acetate	132	156	7.6 (30 °C)	1.8		40.9	28.2	1.025
ethylene glycol	62	198	37.7	2.31	$1.2 \times 10^{-4}$	52.4	46.5	20
formic acid	46	100.8	58	1.41	$6.4 \times 10^{-3}$	23.2	37.67	1.78 (20 °C)
glycerol	92	290	42.5 (25 °C)		$6.0 \times 10^{-6}$		63.3	945
MeOH	32	64	32.6	1.7	$1.5 \times 10^{-7}$	35.3	22.6	0.6
MeAc	74	57	6.7	1.7	$3.4 \times 10^{-4}$	30	24	0.37
PeOH	88	138	13.9	1.7		44.4	25.6	3.347
PrOH	60	97	20.1	1.7	$9.0 \times 10^{-7}$	40.9	23.7	1.72
THF	72	66	7.6	1.75	$4.5 \times 10^{-3}$	27.9	28	0.55
H <sub>2</sub> O	18	100	79.7	1.87	$5.5 \times 10^{-6}$	40.6	72.75	0.89

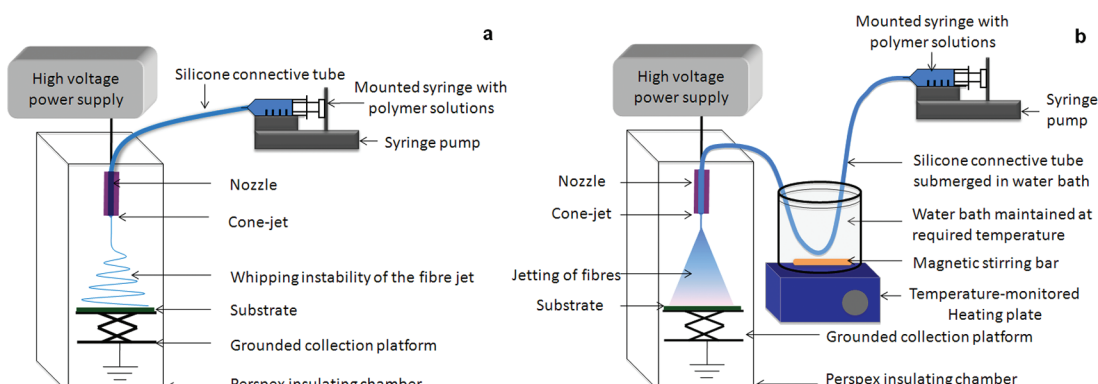


Figure 2. Schematic diagram of an electrospinning setup for (a) materials of ambient temperature and (b) materials of elevated temperature.

comprehensively investigated the influence of dielectric constant over a broad range of solvent systems in electrohydrodynamic processing.<sup>17</sup> This study investigates the influence of solubility and dielectric constant of solvent systems in electrospinning PCL solutions, including the conditions to achieve stable jets, the diameters of the electrospun fibers, the porosity of the fibrous mat, and the productivity of the process. Based on 49 common solvents with diverse solubility parameters and functional groups, the spinnability–solubility map for electrospinning PCL solutions was produced. The solubility behavior of PCL and the electrospinnability of the solutions were correlated. Further, a detailed investigation was carried out with solvents of significantly different dielectric constant but the same functional group and comparable in

other physical properties. In addition, the dissolution and electrospinnability of poor or nonsolvents of PCL at temperatures of 10 °C higher than the ambient temperature (~20–22 °C) were examined, and a unique morphology of electrospun fibers within electrosprayed relicts is produced for the first time.

## 2. MATERIALS AND METHODS

**2.1. Materials.** Poly( $\epsilon$ -caprolactone) (polycaprolactone, PCL,  $M_n = 80\,000$  g mol<sup>-1</sup>) was obtained from Sigma-Aldrich (Poole, UK) and used as received.

Acetic acid, acetone, acetophenone, acetonitrile, benzene, benzene-methanol, bromobenzene, *n*-butanol, butoxyethanol, *n*-butyl acetate (BuAc), carbon disulfide, chloroform ( $\text{CHCl}_3$ ), cresol, cyclobenzene, cyclohexane, cyclohexanol, cyclohexanone, dichlorobenzene (DCB),

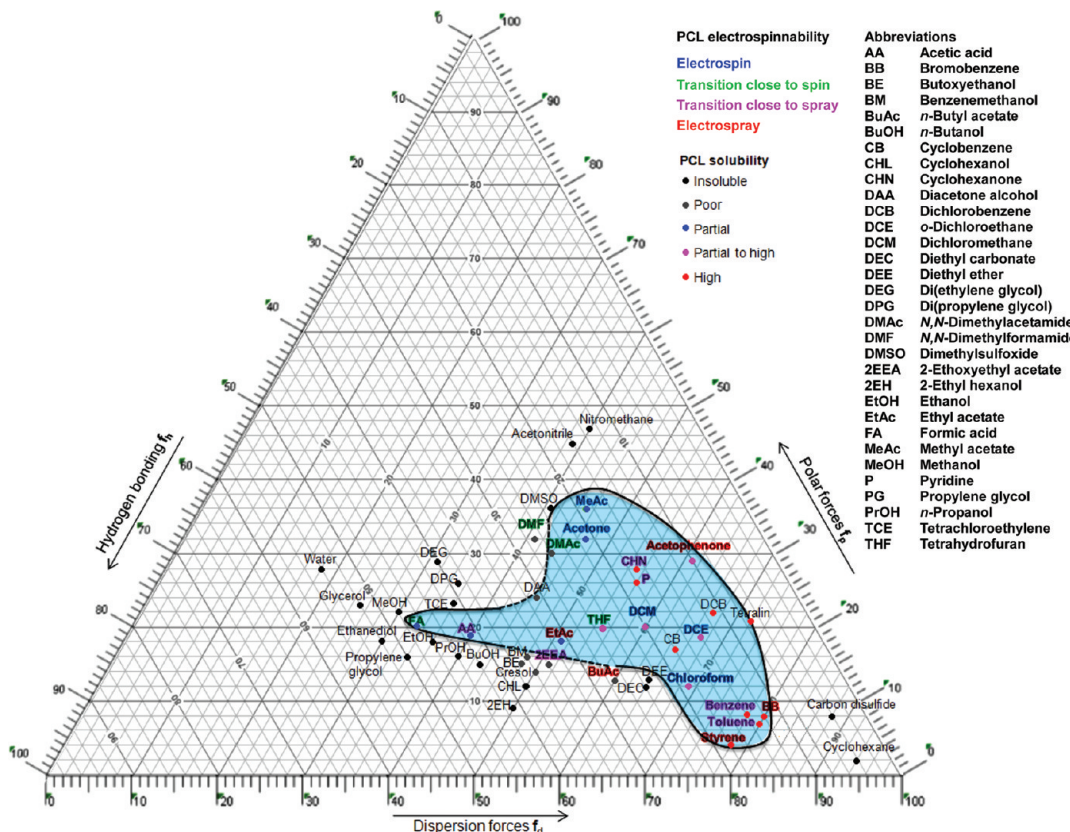


**Figure 3.** Spinnability–solubility map for PCL solution-electrospinning based on the Teas graph, tested at 10% w/w PCL concentration, 1 atmospheric pressure, and ambient temperature of ~20–22 °C. Positions of solvents were based on fractional solubility parameters from Barton.<sup>33</sup> The shaded region enclosed by a contoured outline shows the solubility map of PCL. Dotted lines on this contour indicate the poor solvents on the map shown immediately beyond the shaded region will dissolve PCL and form stable solutions at an elevated temperature of 30 °C.

*o*-dichloroethane (ethylene dichloride/EDC/DCE), dichloromethane (methylene chloride/DCM), diethyl carbonate (DEC), diethyl ether (DEE) diethylene glycol (DEG), dipropylene glycol (DPG), diacetone alcohol, *N,N*-dimethylacetamide (DMAc), *N,N*-dimethylformamide (DMF), *N,N*-dimethyl sulfoxide (DMSO), ethanol (EtOH), 2-ethoxyethanol (Cellosolve), 2-ethoxyethyl acetate (Cellosolve acetate, 2EEA), ethyl acetate (EtAc), 2-ethylhexanol, formic acid, ethylene glycol (ethanediol), glycerol, methanol (MeOH), methyl acetate (MeAc), nitrobenzene, nitromethane, *n*-pentanol (PeOH), *n*-propanol (PrOH), propylene glycol, pyridine, styrene, tetrachloroethylene (TCE), tetrahydrofuran (THF), tetralin, and xylene were obtained from Sigma-Aldrich, Poole, UK. All reagents were of analytical grade and were used as received. Table 1 lists some of the important properties of the major solvents investigated in this work.

**2.2. Mapping Solubility Region of PCL on the Teas Graph.** Solvent positions on the Teas graph are identified by their respective fractional cohesion parameters based on ref 33. The solubility of PCL in solvents diversely positioned on the Teas graph was tested at 10% w/w polymer concentration. The mixture was stirred with a magnetic stirring bar at ambient temperature and pressure (~20–22 °C and 1 atm). The degree of swelling or dissolution was visually assessed after stirring for 10 min, 30 min, 1 h, 2 h, and 24 h. Assessed solubility was categorized and recorded as insoluble, poor, partial, partial to high, and high, based on the time taken for the polymer to dissolve in a solvent to form a homogeneous solution. The results were recorded as insoluble (no dissolution observed after 24 h of stirring), poor (dissolution observed after 24 h of stirring though most solute remained precipitated or in gel form), partial (little dissolution observed after 10 min of stirring, dissolution observed after 30 min of stirring, and complete dissolution observed after 24 h of stirring), partial to high (dissolution observed after 10 min of stirring and

complete dissolution observed after 24 h of stirring), and high (dissolution observed immediately upon mixing and complete dissolution observed after 24 h of stirring). The categorized results were mapped on the Teas graph using different annotation symbols.

**2.3. Mapping the Spinnability–Solubility Graph and Mixing Solvents.** Solvents and solvent systems were selected based on the Teas graph as previously described.<sup>3</sup> Briefly, the proportions of the solvents mixed were geometrically determined based on the Teas graph using a method similar to the lever rule as illustrated by Burke.<sup>34</sup> To do this on the map, a line first joins the positions of two selected solvents (A and B) on the Teas graph. If this line crosses the solubility region of the polymer, a point on this line (P) that falls within a desired solubility and electrospinnability range is identified. The proportions of each solvent component in the system is calculated by volume fraction of solvent A = length of BP/length of AB and volume fraction of solvent B = length of AP/length of AB.<sup>34</sup> The solubility results of mixed solvents using this method were compared to predictions drawn from the Teas graph.

**2.4. Preparation of Polymer Solutions.** Polymer solutions of various concentrations in the unit of percentage by weight (% w/w) were prepared by combining an appropriate mass of the polymer and the solvent system and mechanically stirring for 24 h to obtain homogeneous solutions. In the case of a solution in a binary solvent system, the volume required of each solvent component was measured and the solvents combined. The total mass of the solvent mixture ( $m_s$ ) was weighed, and the mass of the polymer ( $m_p$ ) needed to make the required concentration ( $c$ , in % w/w) of the polymer solution was calculated using the equation

$$m_p = \frac{m_s}{1 - c} c \quad (1)$$

**2.5. Electrospinning Setup.** Polymer solutions were electrospun at ambient temperature using an electrospinning setup shown



**Figure 4.** Photographs showing the visual assessment of the degree of polymer dissolution. (a) No dissolution. (b) Dissolution of some of the polymer. (c) Dissolution of most polymer. (d) Complete dissolution. (e) Dissolution of some polymer, though most solute remained in a precipitated form. A magnetic stirring bar is also seen in the photographs.

in Figure 2a. A stainless steel nozzle of 686  $\mu\text{m}$  inner orifice diameter was connected to a high-voltage power supply (Glassman Europe Limited, Bramley, UK), which generates a DC applied voltage of up to 30 kV. To help maintain the temperature of the solutions in poor or nonsolvents at elevated temperatures, the silicone connection tube was immersed in a water bath contained in a large beaker. The water bath was maintained at the same constant temperature as that of the sample using a hot plate as illustrated in Figure 2b. PCL solutions in 2EEA were processed at 35–50 °C. The water bath was stirred with a magnetic stirring bar to maintain a homogeneous temperature. Care was taken to ensure the silicone connection tube was not in contact with the magnetic stirrer or the bottom of the beaker.

Spinning parameters such as concentration, applied voltage, flow rates, and collection distance were varied to obtain stable jetting condition during electrospinning. Flow rate was controlled by a Harvard syringe pump (Harvard Apparatus Ltd., Edenbridge, UK). Fibers were collected on glass slides and aluminum foils (covering a grounded stainless steel collection platform) for optical and scanning electron microscopy analysis, respectively. Collection duration was fixed at 10 s after 60 s of stable jet spinning. Both materials of ambient temperature and elevated temperatures were electrospun using a single nozzle extruding under ambient air temperature (20–22 °C) and relative humidity (56–65%).

**2.6. Dielectric Constant of Mixed Solvents.** The dielectric constant ( $\epsilon$ ) of a mixed solvent system was calculated based on the work of Wang and Anderko<sup>35</sup> using the  $\epsilon$  value of each solvent component at 20 °C reported in the literature. Mixing two solvents changes the orientation among various polar species. The polarization per unit volume of a fluid ( $p$ ) can be related to the dielectric constant and the refractive index of the solvent. Using Oster's rule,<sup>36</sup> the polarization per unit volume of a fluid mixture of  $n$  components ( $p_m$ ) can be expressed by the mole fraction ( $x_i$ ), the molar volume ( $v_i$ ), and the polarization ( $p_i$ ) of each of the pure component  $i$ :

$$p_m = \frac{\sum_{i=1}^n x_i v_i p_i}{\sum_{i=1}^n x_i v_i} \quad (2)$$

According to the well-known Kirkwood theory<sup>37</sup>

$$p = \frac{(\epsilon - 1)(2\epsilon + 1)}{9\epsilon} \quad (3)$$

Hence,  $\epsilon$  of the mixed solvent system is obtained from eq 3 after the calculation of  $p_m$ .

### 2.7. Characterization of the Electrospun Fiber Morphology.

The morphology of the electrospun fibers was analyzed visually with a Nikon Eclipse ME600 optical microscope, a Hitachi S-3400N scanning electron microscope (SEM), and a field emission JSM-6301F SEM. Each sample was coated with gold using a sputtering machine (Edwards sputter coater S 1 50B) for 60 s prior to observation under the SEM. The gold coating was on both sides if the substrate was nonconductive; otherwise, only the sample-deposited side was coated. The average diameter of the as-spun fibers was determined from the mean value of 25 measurements collected from analyzing the optical and scanning electron micrographs, using an image-processing program UTHSCSA (Image Tool Version 2, University of Texas).

## 3. RESULTS AND DISCUSSION

**3.1. Electrospinning PCL Using the Spinnability–Solubility Map.** Based on 49 common solvents with diverse solubility parameters and functional groups, the spinnability–solubility graph for electrospinning PCL solutions was mapped. The solubility behavior of PCL and the electrospinnability of PCL solutions were correlated and presented in one diagram. The dissolution and electrospinnability of poor or nonsolvents of PCL at temperatures of 10 °C or higher than the ambient temperature were tested and are indicated on the map (Figures 3 and 4).

The spinnability–solubility map of PCL shows solvents topographically located to the bottom right of the ternary graph produce large electrosprayed particles in the micrometer to millimeter range and do not allow electrospinning as single solvent carriers of the polymer. This portion of the graph indicates strong van der Waals forces, strong hydrogen bonding, and weak polar forces (Figure 3). In addition, PCL solutions in solvents of partial to high solubility with moderate dispersion forces frequently showed good electrospinnability.

PCL polymer solutions in single solvent systems of high solubility such as cyclohexanone, acetophenone, benzene, and derivatives of benzene including toluene, bromobenzene, and styrene could not be electrospun into fibers. An examination of the physical properties of these solvents revealed that all of these solvents show at least one of the following properties: high molecular weight, low dielectric constant, low boiling point, strong molecular dispersion forces. PCL solutions in solvents of partial to high solubility such as THF, chloroform, DCE, and DCM formed fibers with diameters in the micrometre range or bead-on-string fibers (Table 2). In addition

**Table 2. Solubility and Electrospinnability Results of 10% w/w PCL in Single Solvent Systems**

solvent	solubility	$\epsilon$ of solvent system (20 °C)	av fiber diam ( $\mu\text{m}$ )	fiber surf. morphology
THF	partial to high	7.6	4.16 ± 1.39	smooth
chloroform	partial to high	4.8	6.67 ± 0.73	smooth
DCM	partial to high	9.1	7.59 ± 0.50	smooth
toluene	high	2.38	droplets	droplets
DCE	partial to high	10.45	3.52 ± 0.77	smooth
FA	partial	58	0.0895 ± 0.0014	smooth
AA	partial	6.2	droplets	droplets

to the relatively high rate of evaporation of these solvents, resulting in fast drying and solidification of the fiber jet during spinning, the relatively moderate dielectric constant value of these solvents can contribute to the larger electrospun fiber diameter. Our previous study on solvent mapping indicated that when the solvents have comparable boiling points, the dielectric constant of the solvent showed a dominant influence on the diameters of the electrospun fibers.<sup>3</sup> Mixing two

**Table 3. Solubility and Electrosprinnability Results of PCL in Mixed Solvent Systems Based on the Adapted Teas Graph**

solvent mixture	v/v ratio	prediction	PCL solubility	electrosprinnability	av fiber diam ( $\mu\text{m}$ )	$\epsilon$ of solvent system <sup>a</sup>
DMAc <sub>poor solvent</sub> :cyclohexanone	high solubility	1:1	partial to poor	poor after standing for 2 h, mixture appeared as a tough colorless gel		
MeOH <sub>nonsolvent</sub> :CHCl <sub>3</sub>	partial to high solubility	3:1	very poor	very poor, little dissolution, PCL pellets showed gel state		
MeOH <sub>nonsolvent</sub> :CHCl <sub>3</sub>	partial to high solubility	1:1	partial	partial	spin	1.19 $\pm$ 0.39
MeOH <sub>nonsolvent</sub> :CHCl <sub>3</sub>	partial to high solubility	1:3	partial	partial	spin	2.28 $\pm$ 0.60
MeOH <sub>nonsolvent</sub> :CHCl <sub>3</sub>	partial to high solubility	1:5	partial	partial	spin	3.65 $\pm$ 0.63
THF <sub>partial to high solubility</sub> :CHCl <sub>3</sub>	partial to high solubility	1:1	partial to high	partial	spin	5.60 $\pm$ 0.44
DMF <sub>nonsolvent</sub> :DCM	partial to high solubility	1:3	partial to high	partial to high	spin	3.54 $\pm$ 0.86
AA <sub>partial solubility</sub> :FA <sub>partial solubility</sub>		3:1	partial	partial	spin	0.0663 $\pm$ 0.0015
AA <sub>partial solubility</sub> :FA <sub>partial solubility</sub>		1:1	partial	partial	spin	0.0828 $\pm$ 0.0014
AA <sub>partial solubility</sub> :FA <sub>partial solubility</sub>		1:3	partial	partial	spin	0.0574 $\pm$ 0.0015

<sup>a</sup>Value of calculated dielectric constant of the mixed solvent system is based on data of solvents at 20 °C (Table 1).

**Table 4. Calculated Dielectric Constant Values and Fractional Solubility Parameters of Some of the Mixed Solvent Systems Used for PCL in the Literature (Data Are Based on Refs 33, 34, 42, and 43)**

mixed solvent system (v/v)	fractional solubility parameters on Teas map			solubility of PCL	$\epsilon$ at 20 °C	ref
	100f <sub>d</sub>	100f <sub>p</sub>	100f <sub>h</sub>			
THF <sub>partial to high solubility</sub> :DMF <sub>nonsolvent</sub> 1:1	47.5	25.5	26.5	partial to poor	23.9	14, 39
MeOH <sub>nonsolvent</sub> :CHCl <sub>3</sub> partial to high solubility 1:1	48.5	17	34.5	partial to poor	18.7	18
DMF <sub>nonsolvent</sub> :DCM <sub>partial to high solubility</sub> 1:4	55.4	23.2	20.4	partial	12.1	40
DMF <sub>nonsolvent</sub> :DCM <sub>partial to high solubility</sub> 4:1	44.6	29.8	21.6	partial	30.5	41

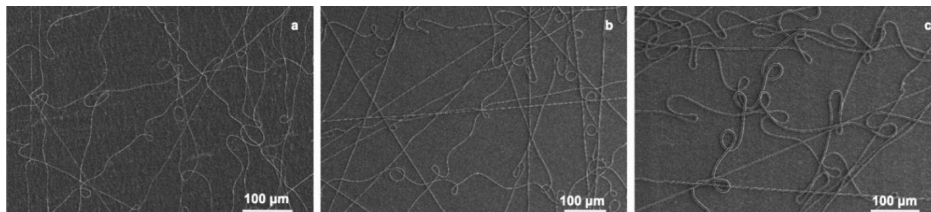


**Figure 5.** Scanning electron micrographs of fibers electrospun at 50  $\mu\text{L}/\text{min}$  under stable jetting conditions from 10% w/w PCL solutions in (a) 1:1 v/v MeOH:chloroform; (b) 1:3 v/v MeOH:chloroform; and (c) 1:5 v/v MeOH:chloroform.

electrospinnable solvents of moderate dielectric constant values, THF and chloroform (Table 3), produced resultant fibers of average diameter  $5.60 \pm 0.44 \mu\text{m}$ —a value close to the average of the respective fiber diameter obtained from each of the single solvent system (THF:  $4.16 \pm 1.39 \mu\text{m}$ ; chloroform:  $6.67 \pm 0.73 \mu\text{m}$ ). Reneker et al. electrospun 14–18% PCL ( $M_w = 80\,000 \text{ g/mol}$ ) in a partial solvent, acetone.<sup>38</sup> The resultant PCL fibers merged and formed garland-like fibrous structures. Similar structures in the same solvent system of 10% w/w PCL of the same molecular weight were observed at 100 mm collection distance in this work. However, when the collection distance was increased to 150 mm, leaving more time for solvent evaporation and drying of the fibers before reaching the collecting substrate, the phenomenon disappeared and dry fibers with little fusion at fiber junctions were collected.

Solvents of varying solubility and dielectric constant were mixed, the dielectric constants of the mixed solvent systems were calculated, the electrospun fibers were characterized, and the average diameters of the fibers were calculated (Table 3). The proportion of a nonsolvent, MeOH, was changed in a PCL solution mixing chloroform (partial to high solubility) and MeOH. This changes the solubility parameter as well as the dielectric constant of the solvent system. MeOH has a low

molecular weight and a high dielectric constant. As the dielectric constant of the solvent mixture increased, the as-spun fiber diameter of the corresponding PCL solutions decreased (Table 4 and Figure 5). Further, an addition of 25% v/v DMF to PCL in DCM also reduced the fiber diameter by more than half (Table 3). A solvent system of PCL mixing 1:1 v/v THF:DMF has been frequently used in tissue engineering for electrospinning PCL nanofibrous scaffolds with average fiber diameters between 500 and 900 nm.<sup>14,39</sup> Shin et al.<sup>18</sup> spun 10% w/w PCL in 1:1 proportion of chloroform and methanol (MeOH) and obtained a nanofibrous mesh with average fiber diameter of 250 nm and a large fiber diameter distribution range of 0.1–5  $\mu\text{m}$ . 8% w/w PCL ( $M_w = 80\,000 \text{ g/mol}$ ) in solvent system DCM:DMF 1:4 or DCM:DMF 4:1 has been reported to allow electrospinning.<sup>40,41</sup> The addition of 10% v/v DMF, a nonsolvent of high dielectric constant for PCL in chloroform, produced beaded nanofibers with diameters  $\sim 150 \text{ nm}$ . DMF additions also produced fibers with narrower diameter distribution profiles.<sup>16</sup> Table 4 provides the calculated dielectric constant values of various mixed solvent systems in the literature.

**3.2. Influence of Dielectric Constant of Two Solvents of Otherwise Comparable Properties.** To examine the

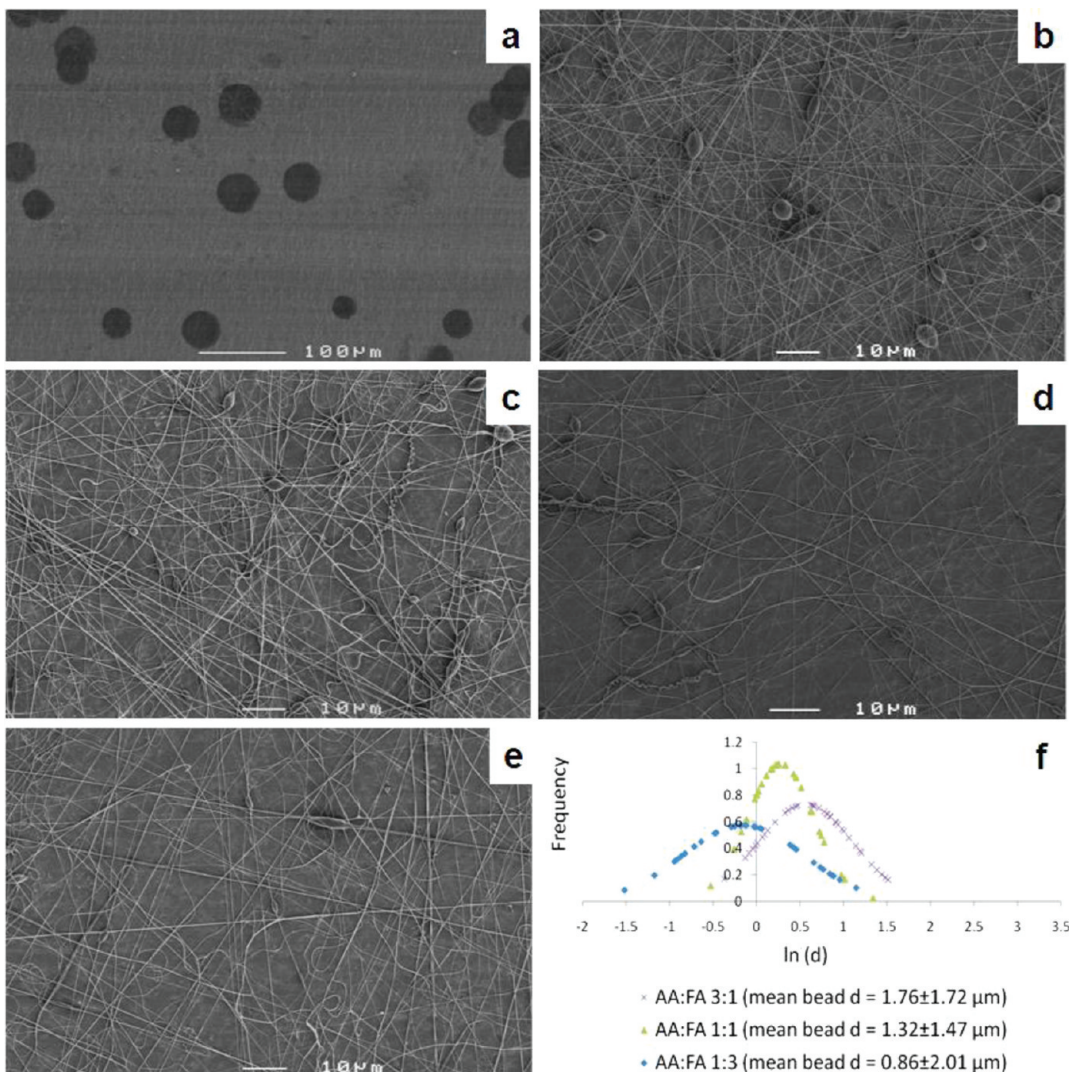


**Figure 6.** Electrosprinnability and bead-on-string profile of solvent systems of acetic acid (AA) and formic acid (FA). (a–e) Scanning electron micrographs of the electrospun products: (a) pure AA, (b) AA:FA 3:1, (c) AA:FA 1:1, (d) AA:FA 1:3, and (e) FA. (f) Log-normal distribution profile of the size and frequency of the beads observed in mixed solvents.  $d$  denotes diameter.

influence of dielectric constants between solvents of a polymer, the solvents to be compared must not only differ significantly in their dielectric constant values but also be similar in terms of the physical properties that are influential in electrospinning, including the functional group of the solvent, the molecular interactions (dispersion forces, polar forces, and hydrogen bonding), solubility, molecular weight, boiling point, latent heat of vaporization, viscosity, and surface tension. Acetic acid and formic acid were the only solvents of PCL found to be suitable for such a comparison (Table 1 and Figure 3). The proportions of the two solvents were calculated to produce solvent systems with a range of dielectric constant values. Both acetic acid and formic acid showed partial solubility for PCL in our solubility test. Numerical values of the Hildebrand solubility parameters reported for both acetic acid and formic acid are close to that reported for PCL ( $10\text{ (cal/cm}^3)^{1/2}$ ),<sup>44</sup> although formic acid is a slightly poorer solvent ( $12.15\text{ (cal/cm}^3)^{1/2}$ )<sup>45</sup> than acetic acid ( $10.35\text{ (cal/cm}^3)^{1/2}$ ).<sup>45</sup>

7% w/w PCL solutions were tested to investigate the significance of the dielectric constant on the electrosprinnability of the solutions, in particular, the influence of the changing proportion of the solvents on the transition from electro-

spraying to electrospinning. The binary solvent systems were electrospun immediately after 24 h of stirring to minimize the influence of acid-catalyzed hydrolysis of the ester bonds of PCL in the solvents.

Changing the dielectric constant of the acetic acid and formic acid solvent system by varying the solvent proportions showed improved electrosprinnability and decreased frequency of bead-on-string formation and decreased diameter of the beads as the dielectric constant of the solvent system increased (Figure 6). Beading in formic acid was infrequent (an average of 2 beads per unit area of  $0.02\text{ mm}^2$ ), and the beading profile was not similar and hence not compared with the mixed solvent system.

The productivity of the electrospinning process for the solvent systems mixing acetic acid and formic acid was not significantly affected by the changing dielectric constant value within the solvent systems investigated, and the mass of the fiber mat collected on the aluminum foil per unit time was similar. However, the interfiber spacing increased and the fiber mat porosity increased. This was presumably due to the increase in the dielectric constant of the solvent. The amount of electrical energy stored in the liquid by the applied voltage increased with increasing dielectric constant of the solvent

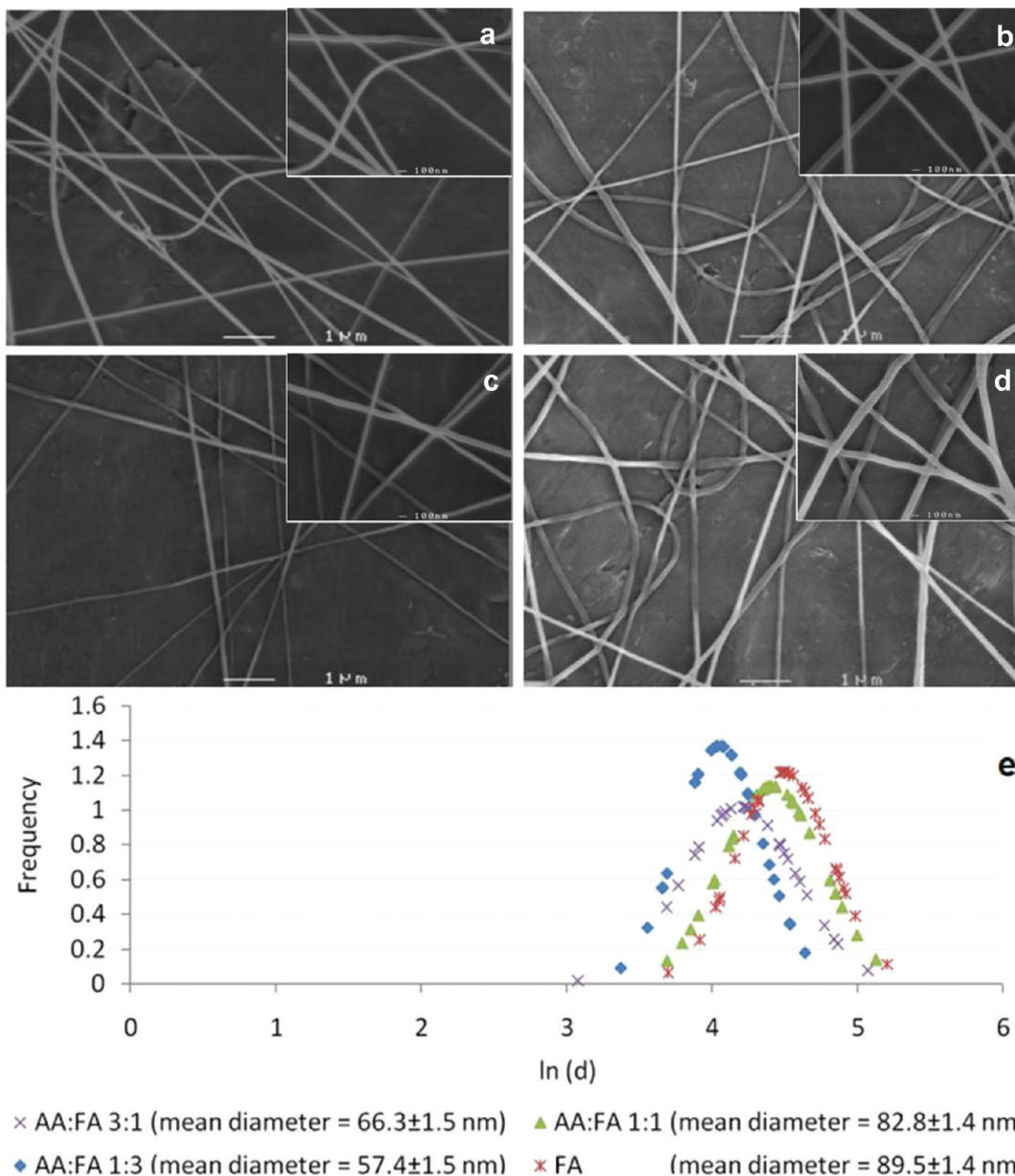


**Figure 7.** Fiber diameter distribution profiles obtained from solvent systems mixing acetic acid and formic acid. (a–d) Scanning electron micrographs of the as-spun fibers from solvent systems of (a) AA:FA 3:1 (mean diameter  $66.3 \pm 1.5$  nm), (b) AA:FA 1:1 (mean diameter  $82.8 \pm 1.4$  nm), (c) AA:FA 1:3 (mean diameter  $57.4 \pm 1.5$  nm), and (d) FA (mean diameter  $89.5 \pm 1.4$  nm). (e) Log-normal distribution profile of the fiber diameters obtained from each solvent system;  $d$  denotes diameter.

system, resulting in larger residual charge and a longer time for the charge to dissipate. Hence, the interfiber spacing increased (Figure 6b–e). This influence of the dielectric constant value may be important for the control of electrospun fiber mat porosity, an important control parameter for cell seeding and the degree of cellular penetration into an electrospun scaffold for tissue engineering.

The addition of calculated proportions of solvents with varying PCL solubility and dielectric constants showed the direct correlation between electrospinnability and dielectric constant. Electrospinning of nanofibers from PCL solutions was achieved when the dielectric constant of the solvent system at  $20^\circ\text{C}$  was in the range of  $\sim 19$  and above (Figures 7 and 8). Solvent systems with dielectric constants below the aforementioned range either produced fibers with diameters in the micrometer range or electrosprayed relics of diameters in the

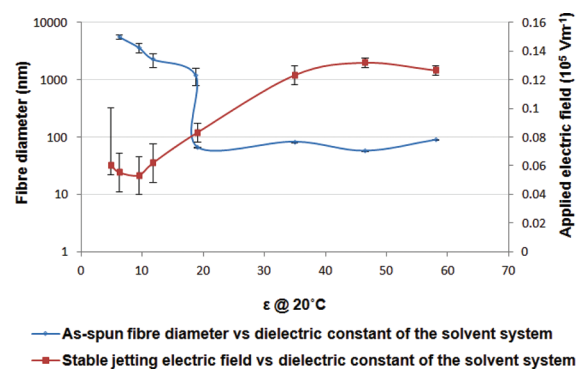


**Figure 8.** Variation in the applied electric field for stable jetting and the electrospun fiber diameter against the dielectric constant of the solvent system.

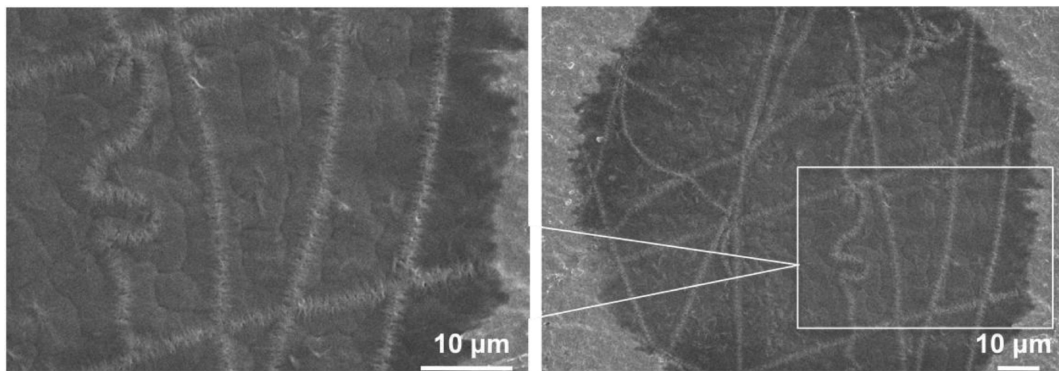


**Figure 9.** Scanning electron micrograph showing buckling patterns of the fibers within electrospayed relics. The samples have a thin layer of gold coating. The circular dark area on the micrograph corresponds where an electrospayed PCL in 2EEA droplet was deposited. The light gray area is the aluminum substrate.

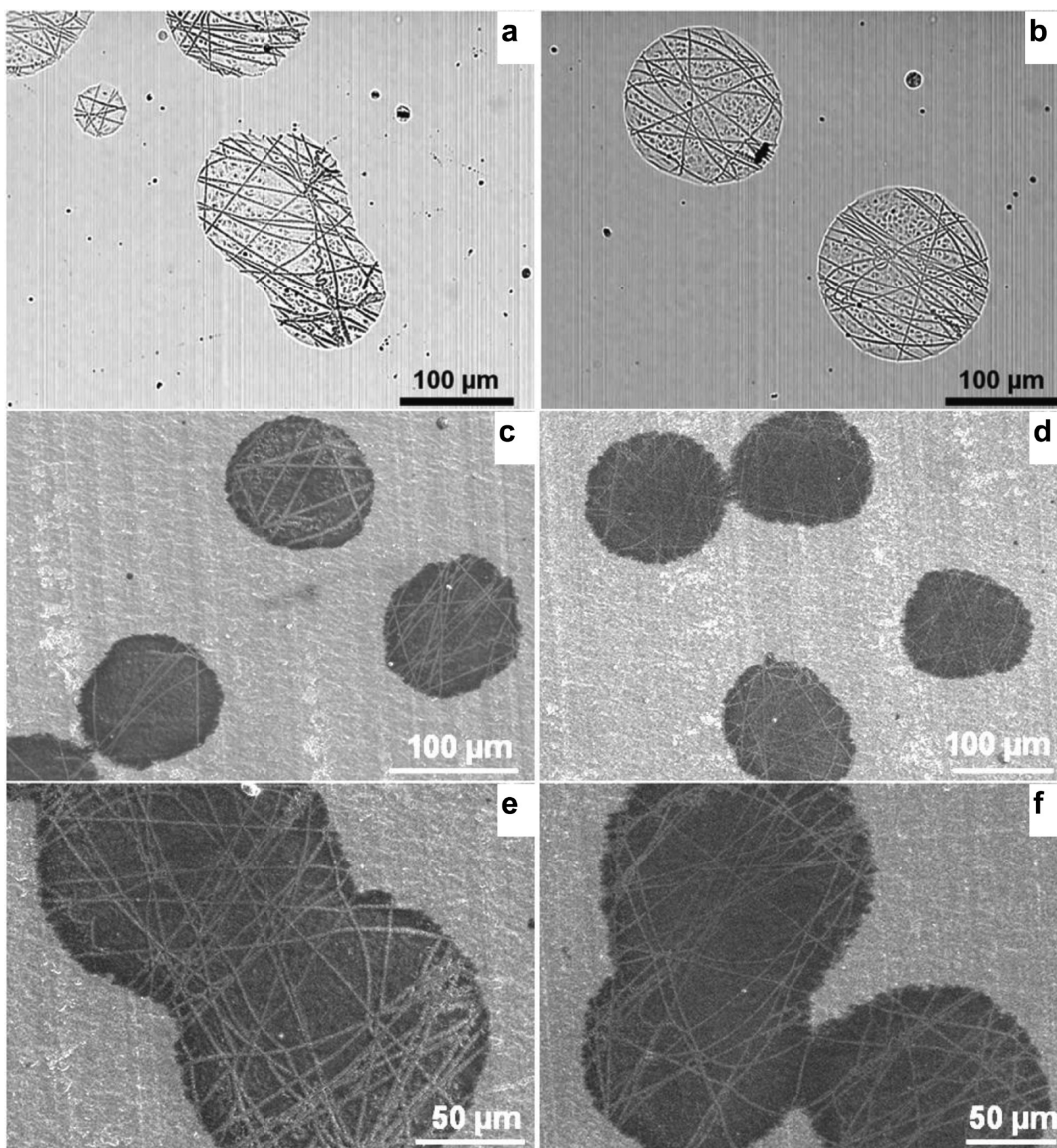


**Figure 10.** (a, b) Optical and (c–f) scanning electron micrographs of fibers from 10% w/w PCL solutions in 2EEA solvent system with an initial spinning temperature of 35 °C.

micrometer to millimeter range. As dielectric constant  $\epsilon$  indicates the ability of a material to become electrically polarized and store electrical energy,<sup>46</sup> a solvent system with

a high dielectric constant is a strong supporter of an applied electrostatic field. It is not surprising that the electrostatic field strength required for stable jet formation increased with the

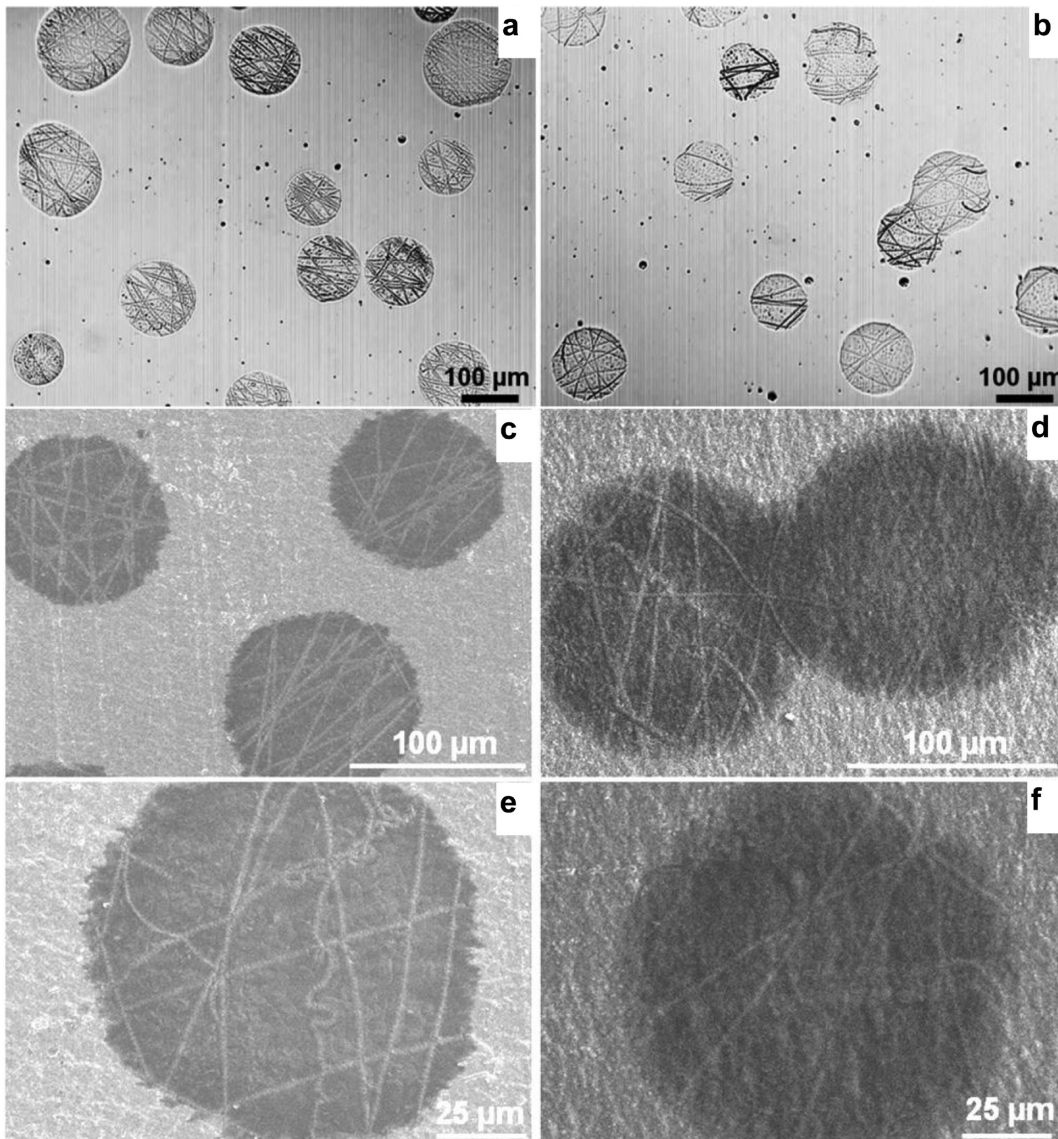


**Figure 11.** Decreased fiber formation as the initial spinning temperature of 10% w/w PCL solutions in 2EEA solvent system increased from 35 to 50 °C: (a) optical and (c, e) scanning electron micrographs of fibers from solutions at 35 °C; (b) optical and (d, f) scanning electron micrographs of fibers from solutions at 50 °C. Collections on glass slides (a, b) showed more fiber formation in the relics than collections on aluminum (c–f).

increasing  $\epsilon$  value of the solvent system (Figure 8). With the increasing dielectric constant of the solvent system and the increased required electrostatic field strength to obtain stable jetting, especially when  $\epsilon$  of the solvent system became higher than 35, the jet obtained at higher electrostatic fields appeared more sensitive to ambient changes.

### 3.3. Electrospun Fibers within Electrosprayed Relics.

By manipulating solvent solubility and changing the temperature of the solvent, this work reports for the first time a unique morphology of electrospun fibers within electrosprayed relics. The morphology was produced when electrospinning PCL in 2-ethoxyethyl acetate (2EEA), a nonsolvent at ambient temperature and a partial solvent for PCL at an elevated temperature of above 30 °C. The fibers were obtained within the circumference of the relics under an applied voltage of 7.5 kV, a flow rate of 50  $\mu$ L/min, and a collection distance of 150 mm (Figures 9–11). The fibers observed showed buckling patterns typical of fibers produced via spinning methods.<sup>47,48</sup>

Optical microscopy provided better observation of the results than scanning electron microscopy. The fibers within the relics appeared sensitive to heat in the vacuum chamber of the SEM and observations often saw the relics destroyed after 5–10 min of exposure to the electron beam of the SEM. The average fiber diameter was  $1.58 \pm 0.49 \mu\text{m}$ . In addition, when the temperature of the spinning liquid increased from 35 to 50 °C, the size of the relics did not change significantly, though the formation of fibers within the relics decreased (Figure 11).

Future studies on electrospinning PCL in 2EEA at an elevated temperature should be carried out over a broader range of temperatures, in particular, to investigate how increasing the temperature of the solution close to the melting point of PCL (65 °C) influences the electrospun results. The influence of processing conditions such as collection distance on the electrospun fibers, including the average density of the fibers within the relics, the diameters, and the aspect ratios of the fibers with respect to the circumference of the relics, should

be further investigated. Collection on glass slides (Figure 11a,b) showed more fiber formation within the circumference of the relics than collections on aluminum (Figure 11c–f). The nature and geometry of the collecting substrate, particularly the dielectric properties, are known to affect the packing density or volume density of conventional electrospun fibrous mats.<sup>46,49–51</sup> How the properties of the collector influence the formation of this unique electrospun morphology should be investigated in further detail.

In addition to the temperature of the material, the fiber jetting environment such as humidity and ambient temperature are known to influence electrospinning and the as-spun fiber morphology, in particular, the phase separation process during fiber formation.<sup>3,5,52–55</sup> Using very high-resolution high-speed cameras, further experimental observations and theoretical simulations on the temperature and humidity change and the consequent change in solvent quality in the spinning liquid as well as the cooling/drying process of the relics collected on different substrates should be further investigated. Moreover, a heated syringe pump and a gas chamber with temperature and humidity monitor may be used for electrospinning instead of ambient conditions to understand how changes in the surrounding temperature and humidity influence the electrospun results.

#### 4. CONCLUSIONS

A spinnability–solubility map was developed for electrospinning PCL solutions. Solvent positions on the map are unique and invariable irrespective of the polymer and allow a user to pinpoint solvents of distinct functional groups as well as easily assess the range of solubility parameters and intermolecular forces of the solvents. The map enables geometrical calculations of the optimal proportions of solvents selected for electrospinning mixed solvent systems.

The influence of solvent dielectric constant on electrospinning PCL solutions is mapped. Acetic acid and formic acid, two PCL solvents with significantly different dielectric constants, but the same functional group and comparable in other physical properties influential in electrospinning, were mixed to produce solvent systems with a calculated range of dielectric constants. Electrospun nanofibers from PCL solutions were achieved when the dielectric constant of the solvent system at 20 °C approached 19 and above. Solvent systems with dielectric constants below this value either produced PCL fibers of micrometer diameters or electrosprayed. The applied electrostatic field strength required to obtain steady jetting increased with the dielectric constant of the solvent system.

Unique electrospun fibers were created within electrosprayed relics for the first time when electrospinning PCL in 2-ethoxyethyl acetate at an elevated temperature of above 30 °C. As temperature of the spinning dope increased from 35 to 50 °C, fiber production within the relics decreased. Further work should be carried out to vary the temperatures to the melting point of PCL to observe the influence of the increased temperature on the resultant product morphology. The influence of the collection distance, the nature of the collecting substrate, the spinning environment, and the cooling process for this solvent system should be further studied to better understand the occurrence of this unique morphology.

In addition, the possibility to incorporate nonsolvents such as ethanol or water in a mixed solvent system for PCL using the spinnability–solubility map should be investigated in the future

to develop a more environmentally and physiologically friendly solvent system for this important biodegradable polymer.

#### ■ ASSOCIATED CONTENT

##### ■ Supporting Information

Background information on solubility parameters and the Teas solubility diagram. This material is available free of charge via the Internet at <http://pubs.acs.org>.

#### ■ AUTHOR INFORMATION

##### Corresponding Author

\*Tel +44 20 7679 2193; fax +44 20 7388 0180; e-mail chaojie.luo@ucl.ac.uk.

##### Notes

The authors declare no competing financial interest.

#### ■ ACKNOWLEDGMENTS

The authors thank EPSRC and a UCL Knowledge Transfer & Enterprise Award for supporting their research.

#### ■ REFERENCES

- (1) Augustijns, P., Brewster, M. E., Eds. *Solvent Systems and Their Selection in Pharmaceutics and Biopharmaceutics*; Springer/AAPS Press: New York, 2007.
- (2) Torres, M. F.; Muller, A. J.; Saez, A. E. *Polym. Bull.* **2002**, *47*, 475–483.
- (3) Luo, C. J.; Nangrejo, M.; Edirisinghe, M. *Polymer* **2010**, *51*, 1654–1662.
- (4) Fong, H.; Chun, I.; Reneker, D. H. *Polymer* **1999**, *40*, 4585–4592.
- (5) Megelski, S.; Stephens, J. S.; Chase, D. B.; Rabolt, J. F. *Macromolecules* **2002**, *35*, 8456–8466.
- (6) Zheng, J. F.; He, A. H.; Li, J. X.; Han, C. C. *Macromol. Rapid Commun.* **2007**, *28*, 2159–2162.
- (7) Luo, C. J.; Stoyanov, S. D.; Stride, E.; Pelan, E.; Edirisinghe, M. *Chem. Soc. Rev.* **2012**, DOI: 10.1039/c2cs35083a.
- (8) Branciforti, M. C.; Custodio, T. A.; Guerrini, L. M.; Averous, L.; Suman Bretas, R. E. *J. Macromol. Sci., Part B: Phys.* **2009**, *48*, 1222–1240.
- (9) Luo, C. J.; Stride, E.; Stoyanov, S.; Pelan, E.; Edirisinghe, M. *J. Polym. Res.* **2011**, *18*, 2515–2522.
- (10) Liao, C.-C.; Wang, C.-C.; Chen, C.-Y. *Polymer* **2011**, *52*, 4303–4318.
- (11) Blades, H.; White, J. R.; White, W. R.; Ford, C. Fibrillated strand; United States Patent 3081519, 1962.
- (12) Shin, H.; Samuels, S. L. Flash-spinning polymeric plexifilaments; United States Patent 5147586, 1992.
- (13) Bazilevsky, A. V.; Yarin, A. L.; Megaridis, C. M. *Langmuir* **2007**, *23*, 2311–2314.
- (14) Li, W. J.; Danielson, K. G.; Alexander, P. G.; Tuan, R. S. *J. Biomed. Mater. Res., Part A* **2003**, *67A*, 1105–1114.
- (15) Lee, K. H.; Kim, H. Y.; Khil, M. S.; Ra, Y. M.; Lee, D. R. *Polymer* **2003**, *44*, 1287–1294.
- (16) Hsu, C. M.; Shivkumar, S. *Macromol. Mater. Eng.* **2004**, *289*, 334–340.
- (17) Pham, Q. P.; Sharma, U.; Mikos, A. G. *Biomacromolecules* **2006**, *7*, 2796–2805.
- (18) Shin, M.; Ishii, O.; Sueda, T.; Vacanti, J. P. *Biomaterials* **2004**, *25*, 3717–3723.
- (19) Zhang, Y. Z.; Venugopal, J.; Huang, Z. M.; Lim, C. T.; Ramakrishna, S. *Biomacromolecules* **2005**, *6*, 2583–2589.
- (20) Zhang, Y. Z.; Wang, X.; Feng, Y.; Li, J.; Lim, C. T.; Ramakrishna, S. *Biomacromolecules* **2006**, *7*, 1049–1057.
- (21) Yoshimoto, H.; Shin, Y. M.; Terai, H.; Vacanti, J. P. *Biomaterials* **2003**, *24*, 2077–2082.

- (22) Ratner, B.; Hoffman, A.; Schoen, F.; Lemons, J. *Biomaterials Science: An Introduction to Materials in Medicine*; Elsevier Academic Press: London, 2004.
- (23) Pitt, C. G. Poly( $\epsilon$ -caprolactone) and its Copolymers. In *Biodegradable Polymers as Drug Delivery Systems*; Chasin, M., Langer, R. S., Eds.; Dekker: New York, 1990; pp 71–120.
- (24) Boland, E. D.; Pawlowski, K. J.; Barnes, C. P.; Simpson, D. G.; Wnek, G. E.; Bowlin, G. L. *ACS Symp. Ser.* **2006**, *918*, 188–204.
- (25) Ziabicki, A. *Fundamentals of Fibre Formation: The Science of Fibre Spinning and Drawing*; Wiley: London, 1976.
- (26) Yarin, A. L. *Free Liquid Jets and Films: Hydrodynamics and Rheology*; Wiley: New York, 1993.
- (27) Tadmor, Z.; Gogos, C. G. *Principles of Polymer Processing*; John Wiley & Sons, Inc.: Hoboken, NJ, 2006.
- (28) Colby, R. H.; Fetters, L. J.; Funk, W. G.; Graessley, W. W. *Macromolecules* **1991**, *24*, 3873–3882.
- (29) McKee, M. G.; Elkins, C. L.; Long, T. E. *Polymer* **2004**, *45*, 8705–8715.
- (30) Hiemenz, P. C. *Polymer Chemistry: The Basic Concepts*; Marcel Dekker, Inc.: New York, 1984.
- (31) Sahu, R. P.; Sinha-Ray, S.; Yarin, A. L.; Pourdeyhimi, B. *Soft Matter* **2012**, *8*, 3957–3970.
- (32) Scheffler, R.; Bell, N.; Sigmund, W. *J. Mater. Res.* **2010**, *25*, 1595–1600.
- (33) Barton, A. F. M. *Handbook of Solubility Parameters and Other Cohesion Parameters*; CRC Press Inc.: Boca Raton, FL, 1983.
- (34) Burke, J. Solubility Parameters: Theory and Application. In *AIC Book and Paper Group Annual*, 1984; Vol. 3, pp 13–58.
- (35) Wang, P.; Anderko, A. *Fluid Phase Equilib.* **2001**, *186*, 103–122.
- (36) *A Comprehensive Treatise*; Franks, F., Ed.; Plenum Press: New York, 1973; Vol. 2.
- (37) Kirkwood, J. G. *J. Chem. Phys.* **1939**, *7*, 911–919.
- (38) Reneker, D. H.; Kataphinan, W.; Theron, A.; Zussman, E.; Yarin, A. L. *Polymer* **2002**, *43*, 6785–6794.
- (39) Li, W. J.; Tuli, R.; Okafor, C.; Derfoul, A.; Danielson, K. G.; Hall, D. J.; Tuan, R. S. *Biomaterials* **2005**, *26*, 599–609.
- (40) Yoon, H.; Ahn, S. H.; Kim, G. H. *Macromol. Rapid Commun.* **2009**, *30*, 1632–1637.
- (41) Kim, G. H. *Biomed. Mater.* **2008**, *3*, 025010–1–8.
- (42) Smallwood, I. M. *Handbook of Organic Solvent Properties*; Arnold: London, 1996.
- (43) Riddick, J. A.; Bunger, W. B. *Organic Solvents: Physical Properties and Methods of Purification*; John Wiley & Sons, Inc.: New York, 1970.
- (44) Sarac, A.; Ture, A.; Cankurtaran, O.; Yilmaz, F. *Polym. Int.* **2002**, *51*, 1285–1289.
- (45) Belmares, M.; Blanco, M.; Goddard, W. A., III.; Ross, R. B.; Caldwell, G.; Chou, S.-H.; Pham, J.; Olofson, P. M.; Thomas, C. J. *Comput. Chem.* **2004**, *25*, 1814–1826.
- (46) Andrade, A. L. *Science and Technology of Polymer Nanofibers*; John Wiley & Sons, Inc.: New York, 2008.
- (47) Han, T.; Reneker, D. H.; Yarin, A. L. *Polymer* **2007**, *48*, 6064–6076.
- (48) Chiu-Webster, S.; Lister, J. R. *J. Fluid Mech.* **2006**, *569*, 89–111.
- (49) Mitchell, S. B.; Sanders, J. E. *J. Biomed. Mater. Res., Part A* **2006**, *78A*, 110–120.
- (50) Theron, A.; Zussman, E.; Yarin, A. L. *Nanotechnology* **2001**, *12*, 384–390.
- (51) Li, D.; Wang, Y. L.; Xia, Y. N. *Adv. Mater.* **2004**, *16*, 361–366.
- (52) Casper, C. L.; Stephens, J. S.; Tassi, N. G.; Chase, D. B.; Rabolt, J. F. *Macromolecules* **2004**, *37*, 573–578.
- (53) Dayal, P.; Liu, J.; Kumar, S.; Kyu, T. *Macromolecules* **2007**, *40*, 7689–7694.
- (54) Dayal, P.; Kyu, T. *J. Appl. Phys.* **2006**, *100*, 043512–1–6.
- (55) Lyoo, W. S.; Youk, J. H.; Lee, S. W.; Park, W. H. *Mater. Lett.* **2005**, *59*, 3558–3562.